LATTICES FOR ANTIPROTON RINGS

B. Autin
CERN, Geneva, Switzerland

ABSTRACT: After a description of the constraints imposed by the cooling of Antiprotons on the lattice of the rings, the reasons which motivate the shape and the structure of these machines are surveyed. Linear and non-linear beam optics properties are treated with a special amplification to the Antiproton Accumulator.

1. INTRODUCTION

The design of lattices for antiproton rings, in most cases, is determined by the requirements imposed by the stochastic cooling techniques[1]. The interplay between the lattice properties and the cooling performances is at the heart of this lecture (Fig. 1). However, an antiproton ring is primarily a closed magnetic structure which, obviously, must satisfy the basic conditions of any machine: the beam has to get in and out and stay stable. Moreover, antiprotons can circulate in rings which have not been foreseen for them, such is the case of CERN PS and FERMILAB MAIN RING which accelerate the antiprotons without any change to their lattice structures. They are stored in high energy accelerators which have to be converted into colliders. This implies the design of special insertions in the collision regions but these techniques are not specific to antiproton rings, they are commonly applied to any kind of collider whatever they are p-p, e-p, e^+-e^- or p-$\bar{p}$ and I shall not insist upon them.

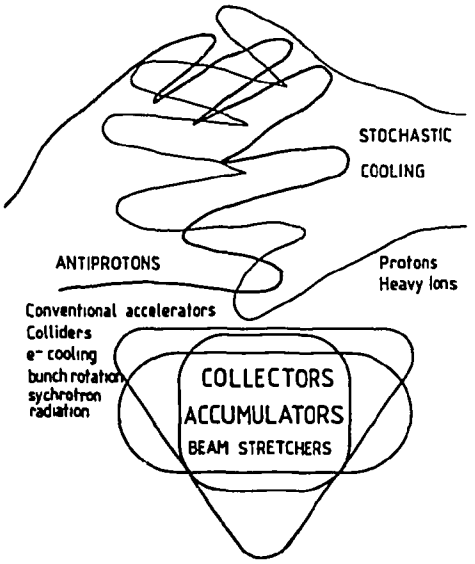

Fig. 1 The marriage of the antiprotons with stochastic cooling.

In order to complete the skyline of antiprotons and cooling, it must be recalled that antiprotons may be cooled by monoenergetic electrons and even, at ultra relativistic energy, by the radiofrequency field which compensates the energy loss due to synchrotron radiation. Last, stochastic cooling can be applied to particles other than antiprotons: protons, neutrons or heavy ions[2]. For heavy ions, laser cooling[3] can be contemplated but its implication on lattice properties have not been studied; I suspect that they are not very stringent

After this digression, I come back to the main topic of this talk which is the study of rings especially built for antiprotons. They belong to three classes of machines.

i. The collectors, also called debunchers or precoolers, receive a burst of antiprotons in a large acceptance and compress the transverse and longitudinal emittances into a phase space volume which is compatible with the input requirements of an accumulator.

ii. The accumulators are storage rings located downstream the collector. The injected beam is captured and transported on a deposition orbit. Then it migrates with all the previously injected pulses towards a "core" whose density is typically four orders of mag-

nitude higher than the density of the injected beam. Once the final density is reached, bunches of antiprotons are extracted from the core and directed towards the users.

iii. The beam stretchers act like buffers between the antiproton source and the physics experiments. They receive an intense burst of particles which spill out of the machine using a method of ultra slow ejection[4].

2. CONSTRAINTS IMPOSED ON THE LATTICE

2.1 General Requirements

2.1.1 Injection-Ejection

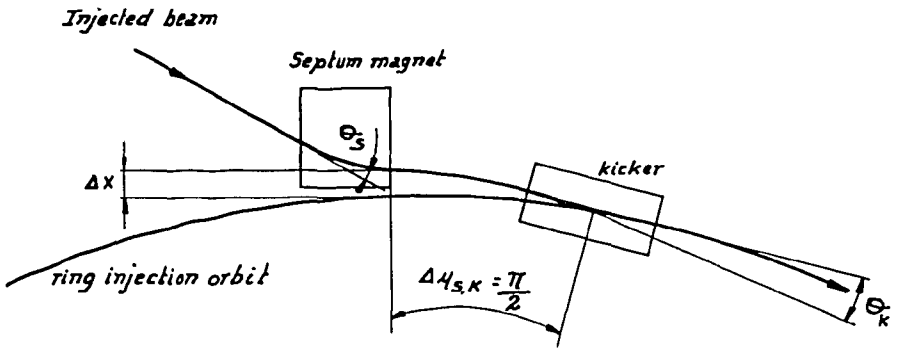

Fig. 2 Injection layout.

A typical scheme of injection is shown in Fig. 2. The injected particles are placed in orbit by adjusting their position and their angle at the entrance to the ring. These two parameters are controlled by two magnets: a "septum" magnet, so called because its aperture on the ring side is closed by a septum of thickness s and a fast deflector, called a "kicker" in accelerator jargon. At the end of the septum magnet, the injection trajectory is parallel to the closed orbit of the ring. The distance between the centre of the beam and the closed orbit is (Fig. 3):

$$\Delta x = D_x \frac{\Delta p}{p} + 2\sqrt{\varepsilon\beta_s} + x_{c.o.} + s \ .$$

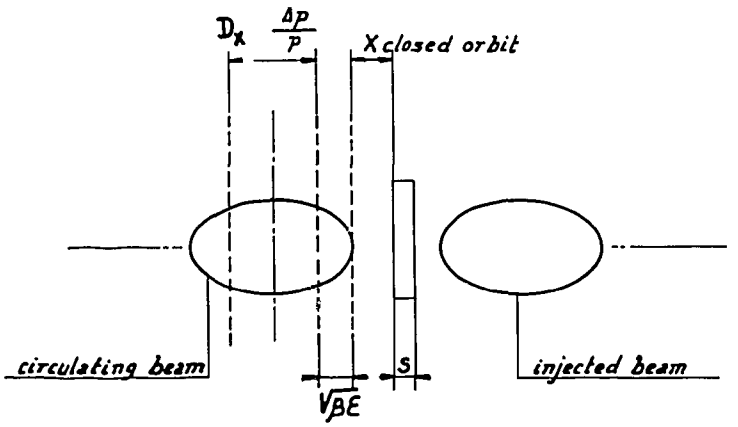

Fig. 3 Beam separation in a septum magnet.

$\Delta p/p$ is the beam momentum spread, ϵ, the beam emittance, D_x, the orbit dispersion and $x_{c.o.}$, the closed orbit distortion. Once the septum magnet is passed, the beam circulates in the lattice of the ring. Being away from the equilibrium orbit by the distance Δx, it undergoes a betatron oscillation which intersects the closed orbit when the betatron phase advance is $\pi/2$ (or an odd multiple of $\pi/2$). At this place, the "kicker" deflects the beam by an angle:

$$\Delta x' = \frac{\Delta x}{\sqrt{\beta_s \beta_k}\, \sin\Delta\mu} .$$

β_s and β_k are the β functions at the septum and kicker, respectively. $\Delta\mu$ is the betatron phase advance between end of septum and kicker. The kicker is a pulsed magnet whose pulse fall time is smaller than the time which separates the instant when the tail of the injected burst of antiprotons leaves the kicker from the instant when the head of the burst comes back in the kicker after one turn. The deflection is minimized when $\sin\Delta\mu$ is equal to 1 and when the value of β_k is high, namely in the neighbourhood of a quadrupole which is focusing in the plane of injection. The beam separation Δx has also to be small; for this reason, the orbit dispersion D_x is close to zero in the septum magnet, the β value is not very relevant at the septum because the kicker efficiency is counterbalanced by the beam width. In a collector, the kicker aperture encompasses all the beam and the orbit dispersion is zero in the kicker. In an accumulator, the kicker acts on the injected beam only and its stray field is shielded by a shutter in order to avoid any disturbance of the stored beam. As the injection is horizontal and the particles are stored in the momentum space, the momentum acceptance of the shutter is:

$$\frac{\Delta p}{p} = \frac{s}{D_x} ,$$

and D_x must be as high as possible at the kicker.

2.1.2 Stability

The stability criterion for small amplitude oscillations is:

$$\mathrm{Tr}(M) < 2$$

where M is the transfer matrix of a superperiod of the ring. A general and precise criterion for large amplitude stability does not exist and it is necessary to resort to numerical computations (see par. 5.3) to track the particles over many turns and make sure that they stay inside the aperture.

Another aspect of beam stability concerns the coherent oscillations induced by space charge forces. Whenever it is possible, the betatron oscillations have a tune which differs from one orbit to the other (finite chromaticity). However, it is an experimental fact that non-linear resonances are dangerous up to a high order and that the working area in the Q_H - Q_V diagram is very restricted. The chromaticity is therefore close to zero and instabilities may build up in the antiproton stack of an accumulator; they are cured by an active feedback using pick-ups and dampers exactly as in a stochastic cooling system but at low frequency (a few tens of megahertz).

2.2 Collision Rings

The performance of a collider is defined by its luminosity L which is given by the relation

$$L = \frac{N_p N_{\bar{p}} B f_0}{4\pi A}$$

in the case of bunched beams circulating on the same orbit. N_p and $N_{\bar{p}}$ are the number of protons and antiprotons per bunch, respectively, B is the number of bunches, f_0 the revolution frequency and A the beam cross-section which is equal to:

$$A = \left(D \frac{\Delta p}{p} + 2\sqrt{\varepsilon_x \beta_x}\right) 2\sqrt{\varepsilon_y \beta_y}$$

A is small if D is zero and β minimum. This leads to the design of low β inserts.

For coasting beams intersecting at the angle α, the luminosity is:

$$L = \frac{1}{ce^2} \frac{I_p I_{\bar{p}}}{h \tan\alpha/2}$$

and it is only the effective height h and thus the vertical β which matter. The minimum value of β is theoretically determined by the length of the interaction region but it is often limited in practice by the quadrupole strengths and the non-linear problems associated with the multipole fields used to correct the chromaticity.

The beam life time is mainly limited by the beam-beam interaction which is a very powerful driving force of non-linear resonances. Here too, the location of the working area in the stability diagram $Q_H - Q_V$ is very sharp. The total magnitude of the effect is reduced when the beams are decoupled in the idle crossing regions. The decoupling can be obtained by modulating the closed orbit with electrostatic deflectors.

2.3 Electron Cooling

A precise co-linearity between electron and antiproton trajectories requires beams of small divergence circulating in regions of high β value. The electron beam produces several perturbations the most important of which being the shift of the (anti)proton betatron tune due to the strong electron space charge. This tune shift has to be compensated by an appropriate excitation of the quadrupoles of the antiproton ring. Other perturbations are due to the fields which bend and focus the electrons when they merge with the (anti) proton beams (Fig. 4). These fields are of three types: dipole, toroidal,

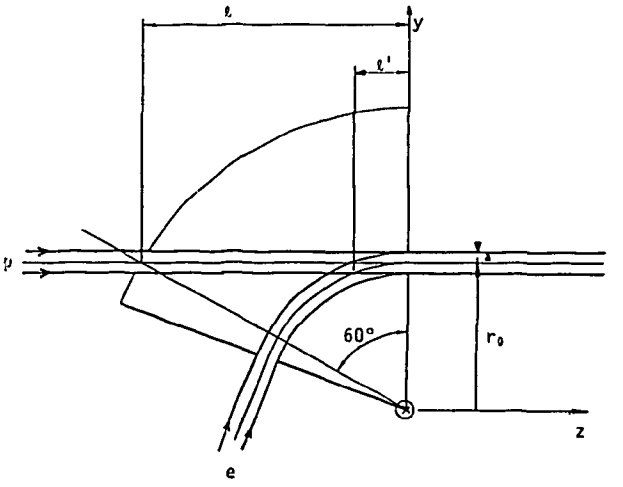

Fig. 4 Interference of electron and proton (or antiproton) beams in an electron cooling machine.

space charge. They create orbit distortions and Q-shifts whose compensation determines the choice of the electron beam layout. In the Novosibirsk arrangement[5], the electrons are injected and ejected on the same side of the proton beam; at Fermilab[6-7] and CERN[8], the electrons get in below the (anti)proton beam and out above it (Fig. 5).

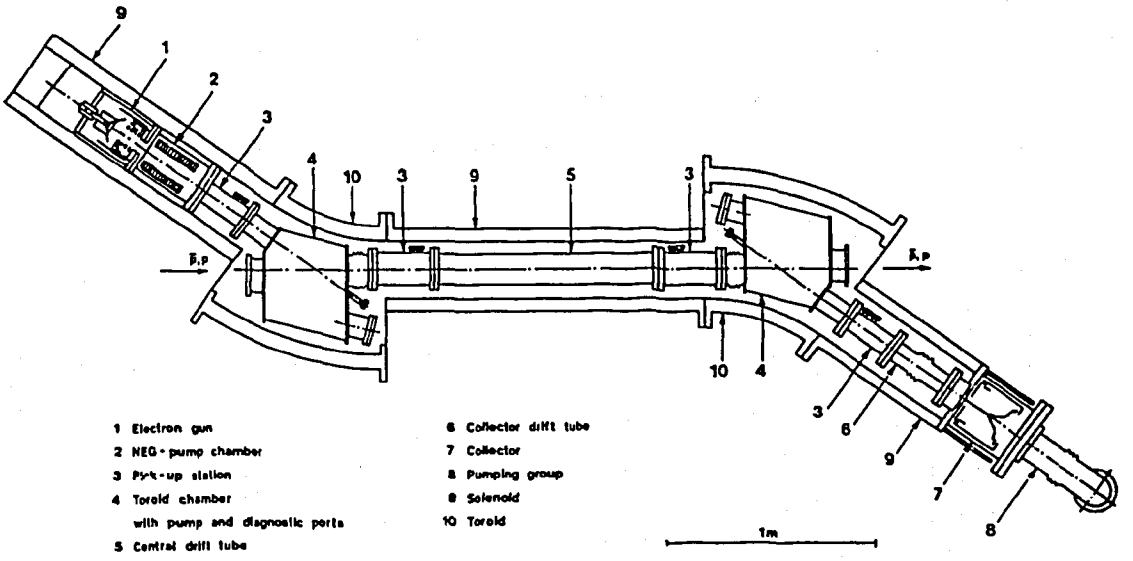

Fig. 5 LEAR Electron Cooler.

2.4 Bunch Rotation

For bunch rotation and for stochastic cooling as well (see section 2.5), an important parameter is the dispersion in revolution frequencies η. The radiofrequency voltage is proportional to η which has to be kept low. For instance, the voltage reaches 4 MV in the Fermilab debuncher for an η value of 0.005. On the other hand, when η is too small, the synchrotron period increases and becomes infinite when η is zero. Once the value of η is chosen for the central orbit, one must make sure that the synchrotron period is uniform over the whole momentum range. This requirement puts a constraint on the sextupole strengths of the lattice (section 5.2.2).

2.5 Stochastic Cooling

2.5.1 "Mixing"

The renewal or the conservation of the particle population in a sample is coined by the term of "mixing" in the theory of stochastic cooling[9]. Figure 6 represents a beam sample observed at two positions under conditions of weak and strong mixing.

The sample observed at a pick-up station must be the same as the sample deflected at a corrector. The variation in revolution frequency for particles of different momenta creates a time lag Δt which corresponds to an RF phase shift:

$$\Delta\phi = \omega \, \Delta t \ .$$

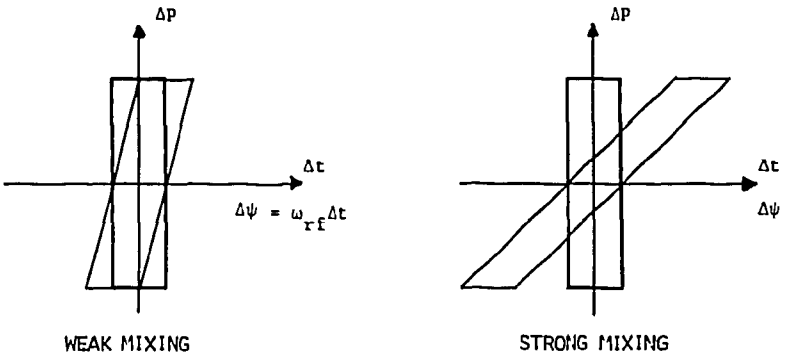

Fig. 6 Evolution of beam samples in the conditions of weak or strong mixing.

It is in general difficult to maintain the coherence of the sample for very high frequencies. However, there may exist regions in the lattice where the phase shift is practically independent of the frequency, i.e. when Δt is close to zero.

The time delay of particles coasting on two extreme orbits is plotted in Fig. 7 for a quadrant of the CERN Antiproton Accumulator. Velocity variations dominate in the first two thirds of the quadrant whereas the steep orbit lengthening in the dipoles where the dispersion is high makes the overall time delay dominated by orbit length variations.

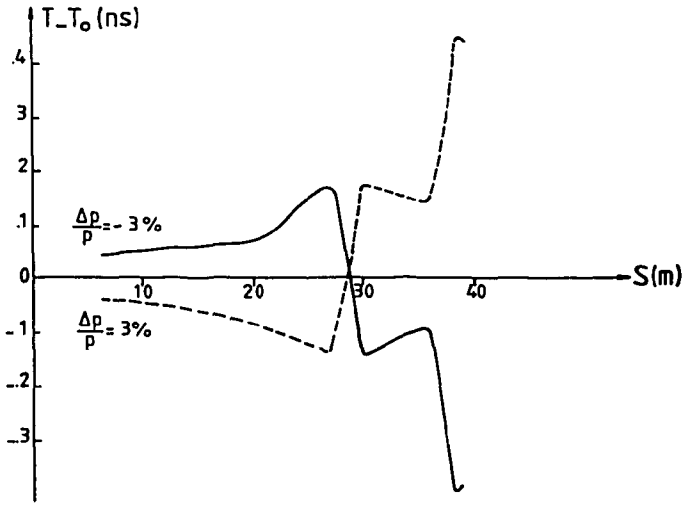

Fig. 7 Differential particle time of flight on two extreme orbits in the Antiproton Accumulator.

Over one turn, the mixing must be incomplete when the cooling is based on the measurement of the revolution frequency. The one-to-one correspondence between momentum and revolution frequency is preserved if the Schottky bands do not overlap. The harmonic number n of the revolution frequency, the momentum byte Δp/p and the η function are then related by the inequality:

$$n \, \eta \, \frac{\Delta p}{p} < 1 \, .$$

When the cooling is based on the measurement of the beam position, the mixing over one turn may be complete.

2.5.2 Betatron Cooling

The considerations developed in the previous section apply to the momentum space; for betatron cooling, the properties of the transverse phase space are those which matter.

The amplitude of the betatron oscillation determines the gap of the electrodes in the stochastic cooling systems and therefore the sensitivity which is inversely proportional to the gap height. A complication occurs when waveguide modes can propagate in the vacuum chamber and one prefers in general to work below the cut-off frequency of the vacuum chamber. In this case, the aperture is smaller than half the cut-off wavelength.

In most betatron cooling systems, the particle position at the pick-up station is converted into an angle at the corrector. For this reason, pick-up and correctors are an odd multiple of a quarter betatron wavelength apart. Whenever it is possible, the systems are located in regions of zero orbit dispersion in order to have a pure betatron signal and a minimum aperture.

Momentum cooling interferes with horizontal cooling when the momentum correctors are located in regions of finite orbit dispersion. Each longitudinal kick produces an orbit jump without changing the particle position so that, after the kick, the particle undergoes a betatron oscillation of amplitude $D(\delta p/p)$ (D: orbit dispersion; p: particle momentum before the kick; δp: momentum correction). When pick-up and corrector are an odd multiple of half betatron wavelengths apart, particles are cooled simultaneously in momentum and in the horizontal plane. When that condition cannot be fulfilled the betatron heating can be avoided with two correctors distant by half a betatron wavelength and sharing the momentum kick equally. Last, in the so-called "zero dispersion" sections, it may be necessary to maintain a quasi-zero orbit dispersion for all momenta, such a condition requires a special scheme of multipole field components (section 5.2.1).

2.5.3 Accumulation

In a stochastic accumulation system[10], the particle density ψ increases exponentially with energy E:

$$\psi = \psi_0 \exp(E/E_d) \ .$$

E_d is a characteristic energy. Such a density profile is obtained by ascribing the system gain G an exponential variation:

$$G = G_0 \exp\left(-\frac{\pi x}{g}\right)$$

where G_0 is the gain corresponding to the initial density ψ_0, g is the half-gap of the pick-up electrodes and x the radial position of the orbits on which the particles are accumulated:

$$x = D_x \frac{\Delta p}{p_0} \ ,$$

the relative variation of momentum is related to the relative variation of energy via the relativistic parameter β:

$$\frac{\Delta p}{p_0} = \frac{1}{\beta^2} \frac{E}{E_0} \ .$$

As the arguments of the exponential functions must be the same in absolute value for the density and the gain, the orbit dispersion and the vertical β function at the pick-up electrodes satisfy the condition:

$$\frac{D_x}{\sqrt{\beta_y}} = \frac{\beta^2 E_0}{\pi E_d} \sqrt{\varepsilon} .$$

For existing accumulators, this condition is fulfilled with a typical value of D_x as large as 10 m.

3. SHAPE OF ANTIPROTON MACHINES

We shall discuss in this chapter the general principles which guide the determination of the length, aperture and architecture of an antiproton machine.

3.1 Length

The minimum length of the ring is the length of the injected antiproton batch. The length of a batch of q equally spaced bunches is the distance between the centres of the first bunch and of a virtual (q + 1)-th bunch (Fig. 8).

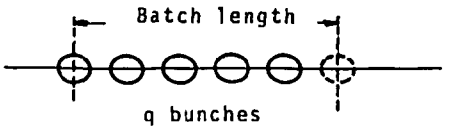

Fig. 8 Particle batch length.

When the bunches are captured by a radiofrequency field, for "bunch rotation" for instance, the RF period is a submultiple of the time separation between consecutive bunch centres. Ring length C and batch length ℓ are then in proportion of two integer numbers:

$$C = \frac{p}{q} \ell, \quad p > q .$$

The choice of p corresponds to the minimum circumference compatible with the magnetic field strength, the antiproton momentum and the length of field-free sections in which the various equipments are accommodated.

3.2 Aperture

The aperture is determined by the number of particles to be accepted and by the focusing structure. The number of particles is proportional to ε^r $(1 < r < 2)$ and to the momentum spread Δp. The focusing structure determines the β function and the orbit dispersion D. The vertical and horizontal apertures are thus given by:

$$A_x = D_x \frac{\Delta p}{p} + 2\sqrt{\varepsilon \beta_x}$$

$$A_y = 2\sqrt{\varepsilon \beta_y} .$$

The concern for small apertures is common to all machines for obvious reasons of economy in construction and power cost. We have seen that the requirements of the stochastic cooling impose very special constraints which favour a strong focusing for the collectors and a weaker focusing for the accumulators although both of them are based on the alternating gradient principles. A precise definition of strong and weak focusing will be given in section 4.1.

3.3 Ring Architecture

The architecture of a machine reflects mainly the æsthetical sense of the designer but it has nonetheless to comply with a number of objective considerations.

The topology has to fit the available space and the connections with the other machines.

The principle of simplicity is generally accepted. It leads to the concept of superperiodicity. The superperiod is the element which, repeated identically to itself a number of times equal to the superperiodicity, defines the machine completely. A superperiod is often symmetric about its midpoint. The higher the superperiodicity, the more regular the machine and the smaller the number of systematic resonances. In an antiproton ring, the trend towards high superperiodicity is tempered by the complexity of the superperiod which is necessarily rather long. Various shapes are drawn in Fig. 9. The "egg" has not been applied in practice but was considered in the development of existing lattices. The "ellipse" was chosen for the AA ring because of its flexibility; the superperiod contains many field free straight sections with a variety of orbit dispersion properties. The record periodicity was obtained with a "pentagon"[11] proposed for the Fermilab $\bar{p}$ source but the "triangle" was finally preferred[12]. The "square"[13] is a shape propitious for negative average orbit dispersion and therefore high dispersion in revolution frequencies and good mixing over one turn.

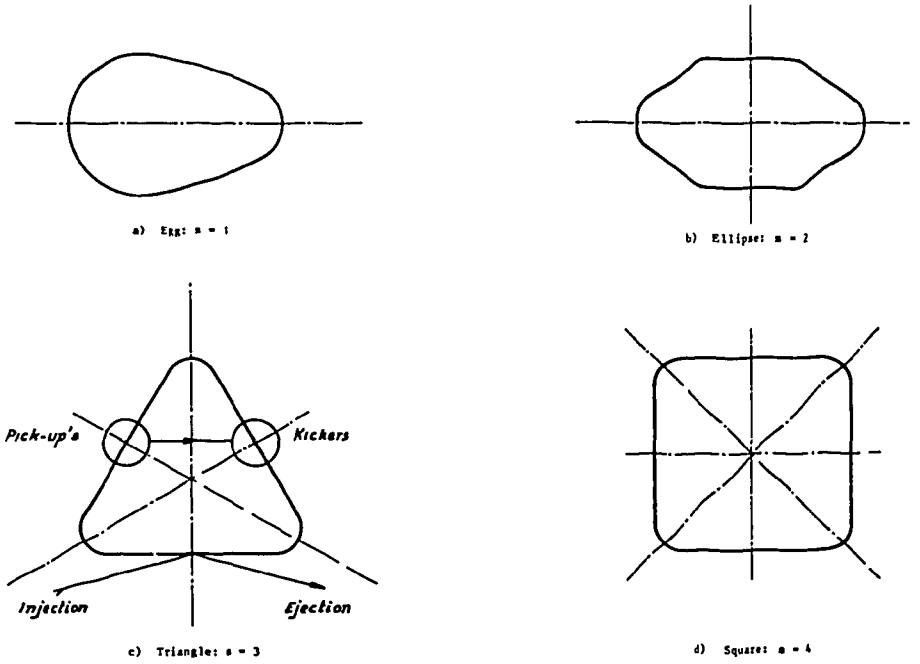

a) Egg: n = 1 b) Ellipse: n = 2 c) Triangle: n = 3 d) Square: n = 4

Fig. 9 Symmetries and superperiodicities.

4. SUPERPERIOD STRUCTURE

4.1 Determination of the Main Characteristics

The main characteristics of a superperiod, like the focusing regime, the tune, the number of cells, the quadrupole strength, etc. can be deduced from a small number of parameters: the machine circumference L, the particle momentum p and the dispersion in revolution frequencies η.

The particle momentum p and the relativistic parameter γ are related by the expression:

$$\gamma = \sqrt{1 + (pc/E_0)^2}$$

where E_0 is the rest energy of the particle. The momentum dependence of the orbit length is defined by the quantity $\bar{\alpha}$:

$$\bar{\alpha} = (dC/C)/(dp/p) .$$

η can thus be expressed by:

$$\eta = \frac{1}{\gamma^2} - \bar{\alpha}$$

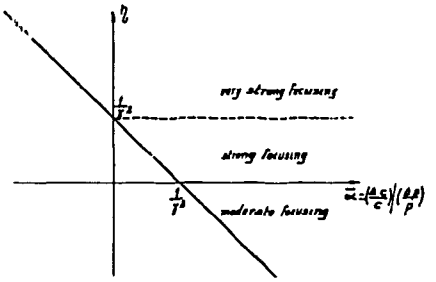

Fig. 10 Focusing regimes.

and is plotted in Fig. 10 for a given value of γ.

The various focusing regimes which have been introduced in section 3.2 can now be defined:

$\bar{\alpha} > 1/\gamma^2$	moderate focusing (Fermilab $\bar{p}$-source, AA)
$0 < \bar{\alpha} < 1/\gamma^2$	strong focusing (ACOL)
$\bar{\alpha} < 0$	very strong focusing (LEAR)

The absolute value of η is prescribed by the bunch rotation in a radiofrequency field and by stochastic cooling requirements. The sign of η is free and has drastic consequences on the magnet system. A strong focusing machine consists of many high gradient quadrupoles with a relatively small aperture. A moderate focusing machine has few low gradient quadrupoles with large apertures. These characteristics will be discussed in the FODO cell section (4.2).

Once η is chosen, $\bar{\alpha}$ is fixed and a first approximation of the horizontal tune is:

$$Q_x \approx \frac{1}{\sqrt{\bar{\alpha}}} .$$

In general, the vertical tune Q_y is close to Q_x since there is a low density of non-linear resonances in the vicinity of the main diagonal of the stability diagram.

The geometry and the phase advance per cell μ_x are determined by the dispersion suppressor (section 4.3) so that the number of cells is:

$$N = \frac{Q_x}{(\mu_x/2\pi)} ,$$

and the length of each cell is:

$$L = \frac{C}{N} .$$

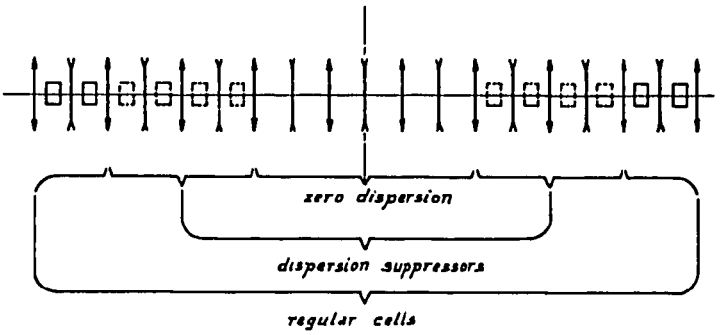

Fig. 11 Superperiod structure.

A typical structure for a superperiod is represented in Fig. 11. It consists of a series of FODO cells with a characteristic orbit dispersion at the ends, no orbit dispersion in the centre and two transition regions, the dispersion suppressors, where the bending magnets are special. Variants of such a superperiod can be obtained by replacing a group of cells by a dedicated insertion. It was implicitly assumed that bending and focusing functions were completely separated between dipoles and quadrupoles. This is only an approximation since the solenoidal component of the field at the end of a dipole introduces a vertical focusing which breaks the symmetry between focusing and defocusing quadrupoles. Last, there is a one-to-one correspondence between orbit dispersion and horizontal tune when orbit dispersion is suppressed with a system of special dipoles. If a separate control of these quantities is wished, extra variables are needed and the quadrupoles next to the zero dispersion sections must have a special strength.

4.2 FODO Cell Parameters

There is a number of ways of building the period of a lattice. The simplest is the FODO cell where focusing and defocusing quadrupoles are regularly alternated with bending magnets (Fig. 12). With respect to other structures like doublets or triplets, the quadrupole strengths are weaker, and the decoupling of the β-functions facilitates the multipole corrections.

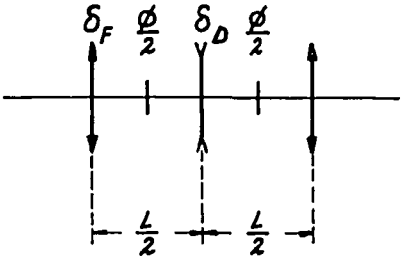

Fig. 12 FODO cell structure.

The theory of this type of cells has already been treated in the literature [14] and its main features only will be reminded here in the framework of the thin lens approximation.

A thin quadrupole is fully defined by a focusing strength δ:

$$\delta = \pm \sqrt{K}\,\ell\,, \qquad \begin{matrix} + : \text{radial defocusing} \\ - : \text{radial focusing} \end{matrix}$$

where ℓ is an equivalent quadrupole length and K is given by:

$$K = \left| \frac{e}{p} \frac{\partial B}{\partial x} \right| .$$

Focusing and defocusing quadrupoles are distinguished by the sign of δ:

$$\delta_F = -\delta_D = -\delta \ .$$

The transfer matrix of a thin quadrupole is:

$$\begin{pmatrix} 1 & 0 & 0 \\ \pm\delta & 1 & 0 \\ 0 & 0 & 1 \end{pmatrix} \ , \qquad \begin{matrix} + : \text{horizontal plane} \\ - : \text{vertical plane} \end{matrix}$$

In a cell of length L, the transfer matrix of each straight section is:

$$\begin{pmatrix} 1 & L/4 & 0 \\ 0 & 1 & 0 \\ 0 & 0 & 1 \end{pmatrix}$$

For a bending magnet of deflection angle $\phi/2$, the matrix is:

$$\begin{pmatrix} 1 & 0 & 0 \\ 0 & 1 & \phi/2 \\ 0 & 0 & 1 \end{pmatrix}$$

The left upper 2×2 matrices are sufficient for betatron computations. The identification of the transfer matrix of a complete cell:

$$\begin{pmatrix} 1 - L\delta/2 - L^2\delta^2/4 & L + L^2\delta/4 \\ -L\delta^2/2 & L + L\delta/2 \end{pmatrix}$$

with its Twiss form, either at an F- or a D- quadrupole,

$$\begin{pmatrix} \cos\mu + \alpha \sin\mu & \beta \sin\mu \\ -\gamma \sin\mu & \cos\mu - \alpha \sin\mu \end{pmatrix}$$

gives:

$$\beta_F = \frac{L}{\sin\mu}\,(1 + \sin(\mu/2)) \qquad \beta_D = \frac{L}{\sin\mu}\,(1 - \sin(\mu/2))$$

$$\alpha_F = -\frac{1 + \sin(\mu/2)}{\cos(\mu/2)} \qquad \alpha_D = \frac{1 - \sin(\mu/2)}{\cos(\mu/2)}$$

$$\delta L = 4 \sin(\mu/2) \ .$$

The β-functions are plotted versus the phase advance per cell μ in Fig. 13. The maximum β-function does not depend very much on μ; therefore, the most efficient way of getting small betatron oscillations for beams of given emittance is to reduce the cell length at the cost of the quadrupole strength.

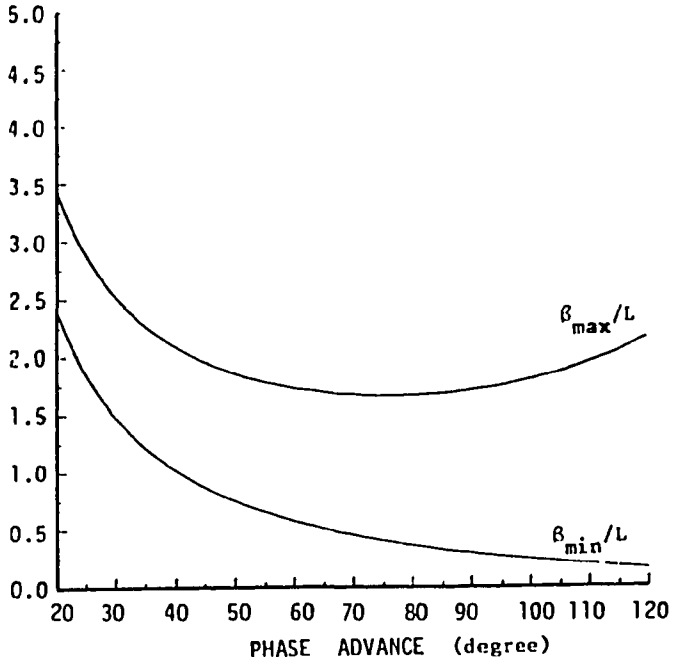

Fig. 13 Maximum and minimum β versus phase advance.

Problem

We have seen that stochastic cooling systems require small apertures. From the above characteristics of a FODO cell, it turns out that a beam of relatively large emittance may have small dimensions in short cells located in dispersionless sections.

Study the following aspects of a string of FODO cells:

1) Matching to the rest of the lattice. Note that an insertion whose transfer matrix is ±I (I: unity matrix) is invisible for the rest of the lattice.

2) Minimum amplitude of the β-functions.

3) Limitations due to quadrupole strengths.

4) Chromaticity correction.

The orbit dispersion D at F- and D-quadrupoles is calculated with the 3 × 3 transfer matrix M of half a cell:

$$M = \begin{pmatrix} 1 - L\delta/4 & L/2 & L\,\phi/8 \\ -L\,\delta^2/8 & 1 + L\,\delta/4 & (1 + L\,\delta/8)\,\phi/2 \\ 0 & 0 & 1 \end{pmatrix} .$$

For a symmetry reason, the derivative of D with respect to the longitudinal coordinate is zero at the quadrupoles. Thus, D_F and D_D result from the solution of the system:

$$\begin{pmatrix} D_D \\ 0 \\ 1 \end{pmatrix} = M \begin{pmatrix} D_F \\ 0 \\ 1 \end{pmatrix}$$

whose first two rows only are independent:

$$\left| \begin{array}{l} D_F = \dfrac{L\phi}{4} \dfrac{1 + 1/2 \sin \mu/2}{\sin^2 \mu/2} \\ \\ D_D = \dfrac{L\phi}{4} \dfrac{1 - 1/2 \sin \mu/2}{\sin^2 \mu/2} \end{array} \right.$$

The orbit dispersion is proportional to the deflection angle and cannot be cancelled in a fully regular structure.

4.3 Dispersion Suppressors

The orbit dispersion can only be suppressed with a special quadrupole or dipole arrangement. The configuration with special dipoles and regular quadrupoles will be discussed in detail because orbit dispersion and betatron oscillations can then be treated almost independently. The decoupling is exact in the horizontal plane when the dipoles are rectangular. However, the vertical focusing is altered by the end field of the dipoles. In other terms, the dispersion-free regions are mismatched with respect to the regular part of the lattice and the vertical β-function is over-modulated unless a special matching procedure is applied. We shall assume that the vertical mismatch can be tolerated and study the beam properties in the horizontal plane only.

The orbit dispersion is cancelled all along a straight section if both the function D and its longitudinal derivative D' are zero at the ends of the dipoles adjacent to the dispersion free straight section. Two deflection angles ϕ_1 and ϕ_2 have to be adjusted in the cells included between the regular cells and the zero dispersion section. Analytical calculations [14-15] have been made for the schemes drawn in Fig. 14. The dispersion vector at the end of a normal cell (section 4.2) is $(D_{F,D}, 0, 1)$. It is tracked through the two special cells characterized by the transfer matrix R. At the end of the dispersion suppressor, it is equal to (0, 0, 1). The calculation of the matrix R is not difficult but very tedious and can be facilitated by algebraic codes [16]. The deflection angles ϕ_1 and ϕ_2 enter the matrix R linearly and are solutions of the system:

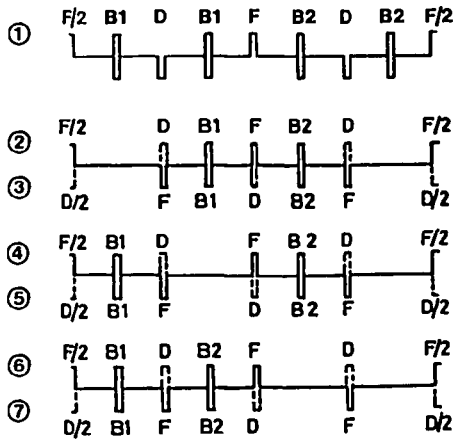

Fig. 14 Seven schemes of dispersion suppressors.

$$R \begin{pmatrix} D_{F,D} \\ 0 \\ 1 \end{pmatrix} = \begin{pmatrix} 0 \\ 0 \\ 0 \end{pmatrix}$$

The results are listed in Table 1 as a function of:

$$\xi = \sin \mu/2 \ .$$

Table 1 - Values of the deflection angles normalized to the regular cell deflection angle for the dispersion suppressors drawn in Fig. 14. ξ is equal to $\sin\mu/2$ for even numbered configurations and to $-\sin\mu/2$ for the odd numbered ones.

Configuration	ϕ_1/ϕ	ϕ_2/ϕ
1	$1 - \frac{1}{4\xi^2}$	$\frac{1}{4\xi^2}$
2, 3	$\frac{(\xi+2)(4\xi^3 - 6\xi^2 - \xi + 2)}{2(\xi^2-2)\xi^2}$	$\frac{(\xi+2)(2\xi^2 + \xi - 2)}{2(\xi^2-2)\xi^2}$
4, 5	$\frac{(\xi+2)(4\xi^3 - 6\xi^2 - \xi + 2)}{2(\xi^2-2)\xi^2}$	$\frac{(\xi+2)(\xi-2)}{2(\xi^2-2)\xi^2}$
6, 7	$\frac{2\xi^2 + \xi - 2}{2\xi^2}$	$\frac{2-\xi}{2\xi^2}$

For special values of the phase advance per cell, one angle can be zero or the two angles can be equal. These special cases are compiled in table 2.

Table 2 - Characteristics of special dispersion suppressors

Configuration	Scheme	$\sin\mu/2$	μ (degree)	ϕ_1/ϕ	ϕ_2/ϕ
1	1	1/2	60	0	1
1	2	$1/\sqrt{2}$	90	0.5	0.5
2	1	0.78078	102.66	1	0
2	2	0.62705	77.67	0	1.42723
3	1	0.55745	67.76	0	1.757
3	2	$1/\sqrt{2}$	90	0.8153	0.8153

Once the ratios ϕ_1/ϕ and ϕ_2/ϕ are known, the condition of orbit closure: sum of deflection angles equal to 2π over one turn, completes the determination of ϕ, ϕ_1 and ϕ_2.

5. NON-LINEARITIES

5.1 Chromaticity

The linear characteristics of a beam are calculated for the orbit which passes through the centre of the quadrupoles. This special orbit is called the "central orbit" for which the particle momentum is p_0. The curvature in the dipoles of field B is:

$$\frac{1}{\rho_0} = \frac{e}{p_0} B \ ,$$

and the focusing strength in quadrupoles of field gradient G is K_0:

$$K_0 = \frac{e}{p_0} G \ .$$

On any other orbit, called "off-momentum orbit", the momentum is:

$$p = p_0 + \Delta p \ ,$$

the curvature:

$$\frac{1}{\rho} = \frac{1}{\rho_0 (1 + \Delta p/p)} \ ,$$

and the focusing strength:

$$K = \frac{K_0}{1 + \Delta p/p_0} \ .$$

The momentum dependence of the curvature and of the focusing strength produces a variation of the orbit dispersion, of the betatron functions and of the betatron tunes. The orbit dispersion will be studied in section 5.2: the betatron functions are calculated with a general optics code but are not subject to a dedicated correction. The variation of the betatron tunes is called the "chromaticity" by analogy with the chromatic aberrations in light optics. The set of couples of values $Q_x - Q_y$ defined over the full momentum range is the "working line" in the stability diagram. Until now, we have only mentioned the focusing perturbations related to the external fields. Space charge forces inside the beam or due to a second beam in the case of colliders and electron cooler may produce important tune variations and the spread in betatron tunes extends over a "working area" in the stability diagram. The discussion is limited here to the external fields.

We have already mentioned in section 2.1.2 the reasons for which the chromaticity has to be corrected. Before describing the correction methods, it is of interest to analyze the various contributions to the natural chromaticity of a machine.

A first contribution comes from the alteration of the focusing strength in the quadrupoles which can be expanded into a power series of the relative momentum error $\Delta p/p_0$:

$$K = K_0 \left[1 - \frac{\Delta p}{p_0} + \left(\frac{\Delta p}{p_0} \right)^2 - \ \ldots \right] .$$

A focusing perturbation induces a first order tune variation:

$$\Delta Q = \frac{1}{4\pi} \int_C \Delta K \ \beta \, ds$$

$$= \frac{1}{4\pi} \left[- \frac{\Delta p}{p_0} + \left(\frac{\Delta p}{p_0} \right)^2 - \ \ldots \right] \int_C K_0 \ \beta \, ds \ .$$

The linear dependence of the tune with $\Delta p/p_0$ is sometimes referred to as the "sextupole" component of the tune because, as we shall see, it is corrected by a sextupole field.

However, this terminology is misleading and must be avoided. There is a basic difference of nature between the kinematic perturbation we have just described and the field perturbation due to a sextupole. For instance, a sextupole field drives a third order resonance but the term $K_0(\Delta p/p)$ cannot do it because the field involved here is simply that of a quadrupole. The same remark applies to higher terms in the expansion of the tune which should be called quadratic, cubic, ... and not octupole, decapole, ...

The integral $(1/4\pi)\int_C K_0 \beta ds$ is practically equal to the tune in machines where quadrupole focusing is dominant. In antiproton machines, we have seen that the orbit dispersion may be deeply modulated and reach values as high as 10 m. The chromatic dependence of the end field may be very important and the natural chromaticity substantially different from the chromaticity of regular machines.

In the hard edge approximation, the edge focusing is represented by the matrix:

$$\begin{pmatrix} 1 & 0 \\ -(1/\rho)\tan\phi & 1 \end{pmatrix}$$

It affects the vertical focusing in a rectangular magnet and the horizontal focusing in a sector magnet. ϕ is the angle of the orbit with the normal to the end face of the magnet

$$\phi = \phi_0 + D' \frac{\Delta p}{p_0} \quad .$$

In a dipole, ϕ_0 is half the deflection angle. The variation of the focusing strength to the first order in $\Delta p/p_0$ is:

$$\Delta\left(\frac{1}{\rho}\tan\phi\right) = \frac{1}{\rho_0}\left(-\tan\phi_0 + \frac{D'}{\cos^2\phi_0}\right)\frac{\Delta p}{p_0} \quad .$$

The longitudinal derivative D' of the orbit dispersion has a very peculiar effect. Let us consider the example of the wide dipole of the antiproton accumulator for which:

$$\rho_0 = 6.49 \text{ m} \; ; \quad \phi = 0.445 \text{ radian} \; .$$

At one end, $D' = -0.81$ and

$$\Delta(1/\rho \tan\phi)/(\Delta p/p_0) = -0.166 \text{ m}^{-1} \; .$$

Inside the magnet, the dispersion increases and reaches the other end with a slope $D' = +0.58$ and we get:

$$\Delta(1/\rho \tan\phi)/(\Delta p/p_0) = +0.059 \text{ m}^{-1} \; .$$

This means that the focusing is reinforced for positive $\Delta p/p_0$. Such an effect is quite exceptional and explains that the horizontal and vertical linear components of the chromaticities are very different in the antiproton accumulator:

$$\frac{dQ_y}{d(\Delta p/p_0)} = 2.3 \frac{dQ_x}{d(\Delta p/p_0)} \quad .$$

The same argument can be repeated for a quadrupole in which case:

$$\phi_0 = 0$$

$$1/\rho = K_0 x$$

$$\simeq K_0 D(\Delta p/p_0)$$

$$\phi = D'(\Delta p/p_0) \ .$$

The variation of the focusing strength is thus mainly quadratic:

$$\Delta(\tan\phi/\rho) \simeq K_0 D D'(\Delta p/p_0)^2 \ .$$

For CERN and Fermilab accumulators, these terms dominate the quadratic variation of the tune.

Such effects do not seem to have been studied before the construction of the antiproton machines. Their importance[17] has stimulated analytical calculations of chromaticity formulae[18, 19] and improvements in the accuracy of general optics programmes.

The above presentation of the fringe field has been based on the "hard edge" model. A treatment of beam optics in an extended fringe field is beyond the scope of this lecture. Well known is the reduction in focusing strength which can be expressed by an angle ε such that:

$$\tan\varepsilon = \frac{b}{6\rho\cos\phi}$$

in the case of a linear fringe field of extension b; $\tan\phi$ has then to be replaced by $(\tan\phi - \tan\varepsilon)$ in the edge focusing matrix. More complicated effects occur when the particle deflection in the fringe field is not negligible with respect to the deflection in the body of the magnet.

The correction of the linear variation of the tune versus $\Delta p/p_0$ requires magnets whose field gradient varies linearly with the orbit position. This type of field is produced by sextupoles:

$$B = \frac{1}{2}\frac{d^2B}{dx^2}x^2 \ .$$

Their focusing strength is:

$$K = \frac{e}{p}\frac{d^2B}{dx^2}x \ ,$$

or, to the first order in $\Delta p/p_0$:

$$K = \frac{e}{p}\frac{d^2B}{dx^2}D\frac{\Delta p}{p_0} \ .$$

Let us put:

$$K' = \frac{e}{p}\frac{d^2B}{dx^2}$$

$$Q' = \left.\frac{dQ}{d(\Delta p/p_0)}\right|_{\Delta p/p_0 = 0}$$

Q' is the wanted linear component of the chromaticity; it results from the sum of the natural term Q'_0 and of the sextupole contribution. To correct the horizontal and vertical chromaticities two families of sextupoles are necessary: one in regions where $\beta_x > \beta_y$, characterized by the variable K'_F, the other in regions with $\beta_y > \beta_x$ and characterized by the variable K'_D. K' values are opposite in horizontal and vertical planes. Let us choose the reference K' in the horizontal plane. The linear system of correction can thus be written:

$$\frac{1}{4\pi}\left\{K'_F \int_C D_F \beta_{x,F}\, dS + K'_D \int_C D_D \beta_{x,D}\, dS\right\} + Q'_{0,x} = Q'_x$$

$$-\frac{1}{4\pi}\left\{K'_F \int_C D_F \beta_{y,F}\, dS + K'_D \int_C D_D \beta_{y,D}\, dS\right\} + Q'_{0,y} = Q'_y \,.$$

Subscripts x and y stand for horizontal and vertical, respectively. Usually Q'_x and Q'_y are made equal to zero for antiproton machines. In a similar way, the quadratic variations of the chromaticity can be corrected by octupole fields:

$$B = \frac{1}{6}\frac{d^3B}{dx^3} x^3$$

whose focusing strength is:

$$K = \frac{1}{2} K'' x^2 \,,$$

with

$$K'' = \frac{e}{p}\frac{d^3B}{dx^3} \,,$$

and

$$x = D\frac{\Delta p}{p_0} \,.$$

The quadratic variation of the chromaticity is defined by the coefficient:

$$Q'' = \left.\frac{d^2Q}{d(\Delta p/p_0)^2}\right|_{\Delta p/p_0=0} \,,$$

and, with the same notations as for the sextupole system of correction, the octupole system of correction can be written:

$$\frac{1}{4\pi}\left\{K''_F \int_C D_F^2 \beta_{x,F}\, dS + K''_D \int_C D_D^2 \beta_{x,D}\, dS\right\} + Q''_{0,x} = Q''_x$$

$$-\frac{1}{4\pi}\left\{K''_F \int_C D_F^2 \beta_{y,F}\, dS + K''_D \int_C D_D^2 \beta_{y,D}\, dS\right\} + Q''_{0,y} = Q''_y \,.$$

In practice, the multipole corrections can be achieved by using genuine multipole magnets, by addition of a given multipole component to the profile of a quadrupole or of a

dipole, or by a change in the effective length of a magnet. In the last case, a parabolic end face of a dipole corrects the linear variation of the chromaticity. Higher multipole components are generally achieved by shaping the end faces of the quadrupoles according to the law:

$$\ell(x) = a \frac{K^{(n)}\, x^n}{K\,(n+1)!}\, \ell_0 \ .$$

ℓ is the magnet effective length, n the order (2 for a quadratic correction of the tune, 3 for a cubic correction, etc.), $(K^n \ell_0)$ the "equivalent" multipole strength of a thin lens and a an efficiency factor (~ 1.6 for AA).

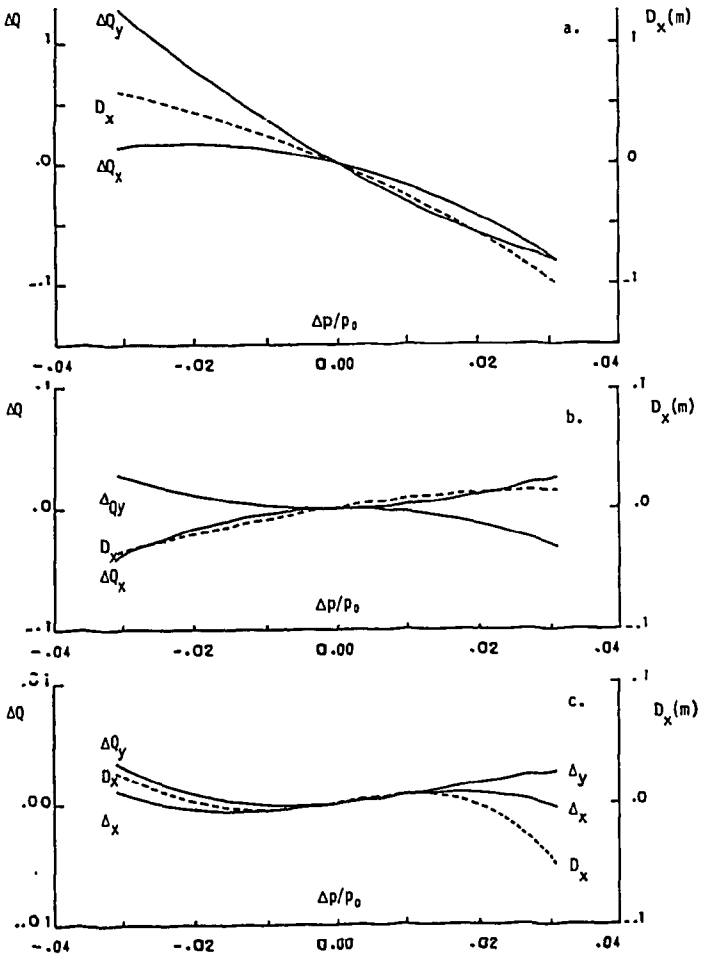

Fig. 15 Tune errors (ΔQ) and horizontal dispersion (D_x) in the CERN Antiproton Accumulator at the design stage: a. Bare machine, b. After sextupolar correction, c. After sextupolar and octupolar correction.

The chromaticity correction of the Antiproton Accumulator[17-20] is illustrated in Figs 15 and 16. The sextupole components were split between the profile of the wide quadrupoles

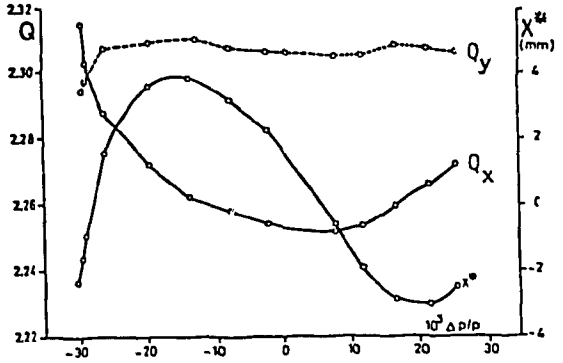

Fig. 16 a. An early measurement of Q_x, Q_y and x*, the position of the beam where α_p should be zero.

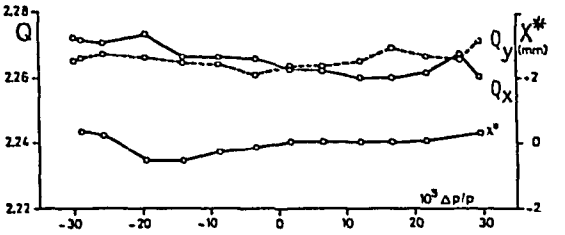

Fig. 16 b. Q_x, Q_y and x* after correction.

and the ends of the dipoles. The higher multipole components were applied to the end faces of the quadrupoles using iron washers distributed along the poles. The correction system consists of three, and not two, families of elements at each multipole level because, in addition to the two chromaticities, the orbit dispersion had to be controlled in stochastic cooling systems (5.2.1).

5.2 Orbit Dispersion Distortion

The control of the orbit dispersion over the full range of momenta is requested in zero dispersion regions to avoid synchro-betatron coupling and in high dispersion regions to adjust the orbit length and therefore the parameter η.

5.2.1 Synchro-Betatron Motion

The expansion of the orbit position in powers of relative momentum errors is:

$$x = D_0 \frac{p - p_0}{p_0} + \frac{1}{2} D_1 \left(\frac{p - p_0}{p_0}\right)^2 + \frac{1}{6} D_2 \left(\frac{p - p_0}{p_0}\right)^3 + \ldots \quad .$$

When a particle of momentum p receives an impulse δp, its position does not change but its closed orbit jumps by an amount:

$$\delta x = D_0 \frac{\delta p}{p_0} + D_1 \frac{p - p_0}{p_0} \frac{\delta p}{p_0} + \frac{1}{2} D_2 \left(\frac{p - p_0}{p_0}\right)^2 \frac{\delta p}{p_0} + \ldots \quad ,$$

and a betatron oscillation is generated. The transfer of energy from a longitudinal kick to a transverse oscillation is the synchro-betatron coupling. It is best avoided by minimizing δx in cancelling as many terms as possible in the above expansion. D_0 is made zero by the dispersion suppressors (4.3). D_1 can be eliminated using a field which has a quadratic dependence on x, of sextupole type (5.1). While chromaticity is corrected by the gradient of a multipole field, the orbit dispersion is corrected by the field itself and the formula of the orbit distortion is to be used:

$$D_n^* + \frac{\sqrt{\beta^*}}{2 \sin(Q\pi)} \int_C \sqrt{\beta_m} \cos\left[-Q\pi + \mu_m(s) - \mu^*\right] D_m^{n+1} K^{(n)} \, ds = 0 \quad .$$

n is the order of correction (1 for sextupole, 2 for octupole, ...), m denotes the multipole element and "*" the point where the orbit dispersion is corrected.

The control of the orbit dispersion imposes an extra condition with respect to chromaticity correction and three families of multipole magnets, at least, are needed at each order of the correction. An example of such a scheme for the AA ring is illustrated in Fig. 17.

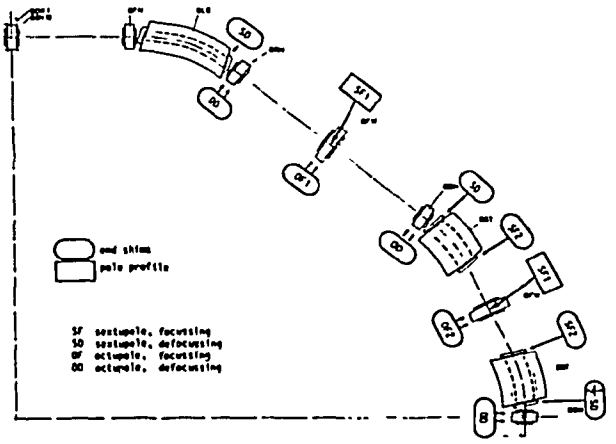

Fig. 17 Multipole corrections in one quadrant of the Antiproton Accumulator

5.2.2 Dispersion in Revolution Frequencies

When the value of the η-function which represents the dispersion in revolution frequencies is small, the particles which drift on off-momentum orbits may become almost synchronous. Under these conditions, the bunch rotation[21] in the momentum space and the "mixing" conditions of stochastic cooling may be seriously affected.

The definition of the η-function is:

$$\eta = \frac{(df/f)}{(dp/p)} \quad ,$$

where f is the revolution frequency. Split into the velocity (or relativistic β parameter) and the orbit length contribution, the expression of η becomes:

$$\eta = \frac{d\beta/\beta}{dp/p} - \frac{dC/C}{dp/p} \quad .$$

The relationship between β and p is:

$$\beta = \frac{pc/E_0}{\sqrt{1 + (pc/E_0)^2}} \quad ,$$

and it is easy to show that, about the central orbit defined for particles of momentum p_0, the expansion of β gives:

$$\frac{d\beta/\beta}{dp/p_0} = \frac{1}{\gamma_0^2} - \frac{3}{2}\frac{\beta_0^2}{\gamma_0^2} \cdot \frac{dp}{p_0} + \ldots \quad .$$

The relative change in circumference can be expressed in terms of the orbit dispersion D and the magnetic radius ρ:

$$\frac{dC/C}{dp/p} = \frac{1}{C} \int_C \frac{D}{\rho} ds \quad .$$

Expanding D and ρ gives:

$$D = D_0 + D_1 \frac{dp}{p_0} + \ldots$$

$$\rho = \rho_0 \left(1 + \frac{dp}{p_0} \right)$$

$$\frac{D}{\rho} = \frac{1}{\rho_0} \left\{ D_0 + (D_1 - D_0) \frac{dp}{p_0} + \ldots \right\}$$

The η-function is then constant to the second order in dp/p_0 if:

$$\frac{1}{C} \int_C \frac{D_1 - D_0}{\rho_0} ds = - \frac{3 \beta_0^2}{2 \gamma_0^2}$$

or

$$\frac{1}{C} \int_C \frac{D_1}{\rho_0} ds = \bar{\alpha}_0 - \frac{3 \beta_0^2}{2 \gamma_0^2} \quad .$$

By introducing the sextupole strengths K' explicitly the above integral becomes:

$$\int_C \frac{D_1}{\rho_0} ds = \int_C \left\{ \int_C \sqrt{\beta(\sigma)} \cos \left[-Q\pi + \mu(\sigma) - \mu(s) \right] D_0^2 K' d\sigma \right\} \frac{\sqrt{\beta(s)}}{2 \rho_0 \sin Q\pi} ds \quad .$$

This form is useful for improving the performance of an existing machine but, at the design level, it is easier to let an optics program optimize the η-function automatically.

The remarks made in the previous section on the number of multipole families and the extension of the procedure to higher orders remain valid here.

The comparison of bunch rotations[22] between machines in which the η function is distorted and uniform is shown in Fig. 18.

5.3 Large Amplitude Stability

Once a sextupole scheme has been established, it has to be checked that particles of large amplitude stay in the machine. The problem is especially crucial for collectors whose acceptances may reach $200\,\pi$ mm.mrad.

A first approach consists of evaluating the width of non-linear resonances[23] driven by the multipole fields introduced for the various chromatic corrections or by magnetic field errors. It is intuitive that the narrower the stopband, the more stable the motion is; it is

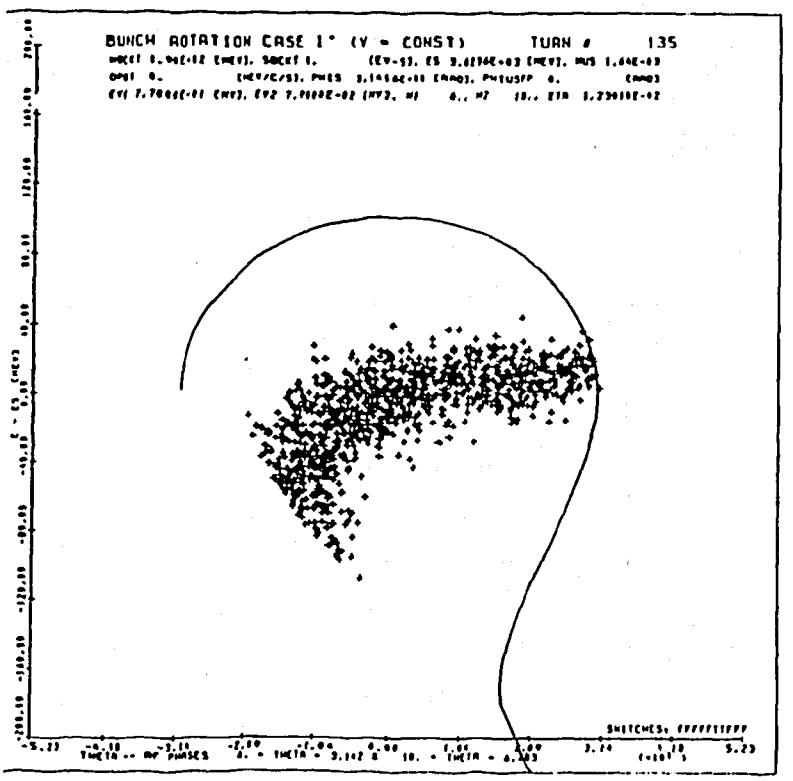

a. Distorted η variation with momentum.

b. Quasi uniform η in the whole aperture.

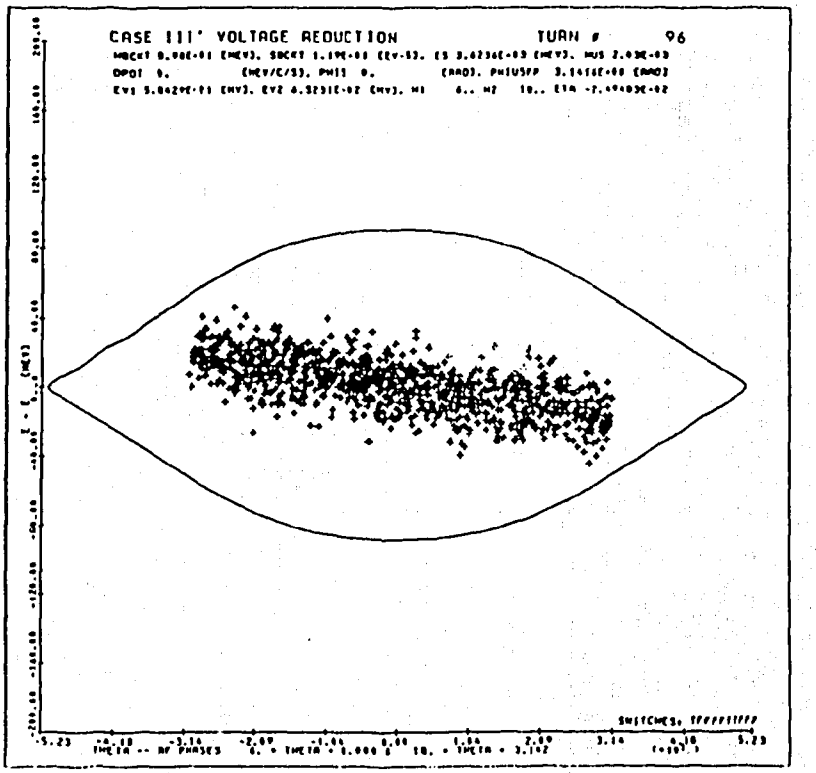

Fig. 18 Bunch rotation.

thus a good recipe to have a multipole scheme which is self-compensated for non-linear resonances. A phase advance of 60° per cell for instance is ideal to suppress third order resonances induced by a set of sextupoles of equal strengths distributed regularly in the lattice; indeed, the phase which is relevant to third order resonances is equal to three times the betatron phase for one-dimension resonances, therefore the excitations induced in two adjacent cells by identical sextupoles are just opposite. If the self-compensation in the multipole scheme is incomplete, one can use sets of multipoles of the same nature in zero dispersion regions to cancel the strongest resonances without altering the chromatic properties of the machine.

The theory of non-linear resonances assumes that a principle of superposition of non-linearities is valid. This is true when there is a negligible cross-talk between the multipoles. However, a coupling exists through the distortion of β- and D-functions produced by the multipoles themselves and it can be dramatic when the multipoles are too strong. In general, this excessive multipole strength occurs in very strongly focusing machines because, on one hand, the natural chromaticity is high, and, on the other hand, the orbit dispersion is too small and the multipole field has no "grasp" on the beam. A practical criterion for multipole strength can be stated: a multipole scheme must be specific of the order of correction it is made for. In the case of chromaticity for instance, the sextupoles must correct the linear momentum dependence of the tune only and not introduce higher order components whose magnitude exceeds the natural kinematic non-linearities of the machine.

A really pathological situation occurs when the condition of "resonance overlap" is fulfilled[24]. Although the stopbands cannot overlap[25], this condition is considered as a frontier beyond which the particle motion is stochastic.

Ultimate checks of particle stability at large amplitude are made with tracking programs[26] where multipole fields are often idealized in the form of thin lenses in which the particle position remains unchanged while the angle is increased by the quantity:

$$\Delta x' = (K^{(n)} \ell) \frac{x^{(n)}}{n!} .$$

Particles of given position, angle and momentum are launched in the lattice and turn a few hundreds of turns. Their coordinates in the transverse phase planes (x-x'), (y-y') are plotted at each revolution (Fig. 19). If phase space plots are quasi-elliptical, we "believe" in long term stability; if they are noticeably different, the multipole scheme is revised. It is true that there is an act of faith in this method because it is perfectly conceivable that a non-linear effect remains latent during many turns and produces a dramatic amplitude increase after a relatively long time. A theoretical breakthrough is certainly needed in the domain of non-linear dynamics. In the mean time, we have to manage with existing computing tools keeping in mind that nature may be a source of trouble but may also be forgiving since, experimentally, proton or antiproton beams have been stored many hours and even days without an excessive deterioration.

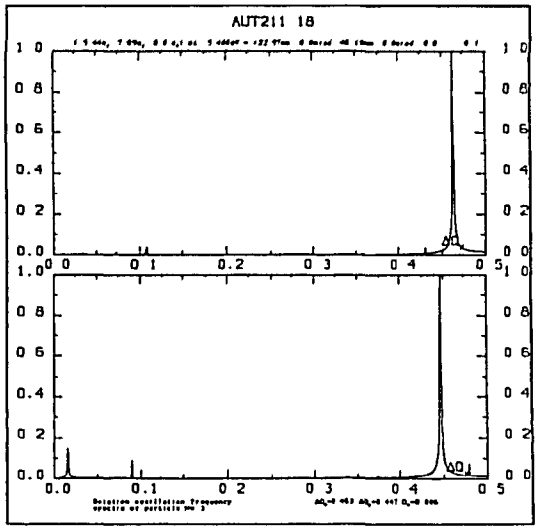

a. Spectrum of betatron oscillations

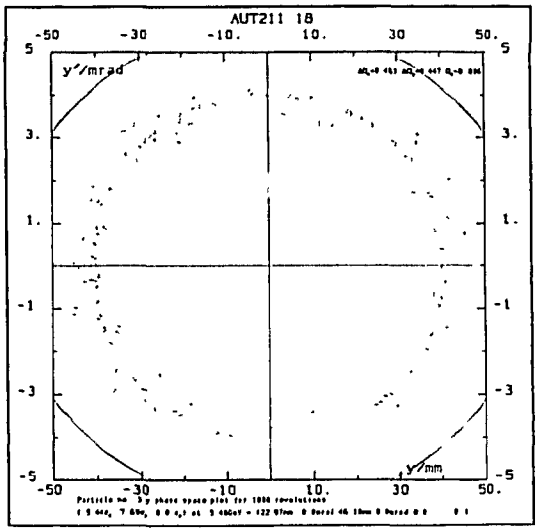

b. Horizontal phase plane

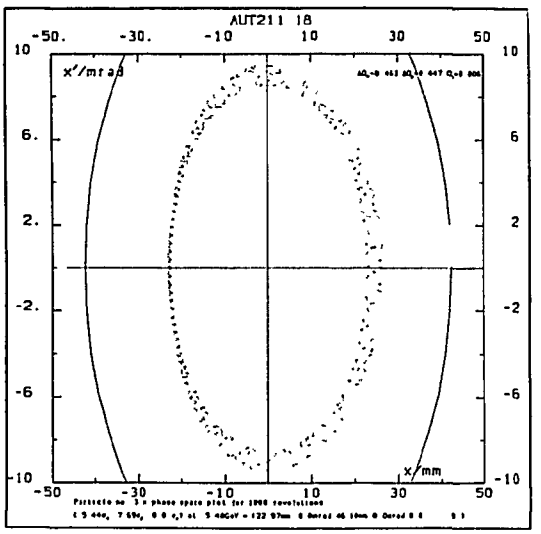

c. Vertical phase plane

Fig. 19 Example of particle tracking in an antiproton ring (ACOL).

6. AN EXAMPLE OF ANTIPROTON RING: THE ANTIPROTON ACCUMULATOR (AA)

The Antiproton Accumulator[27] is a storage ring of 50 π m diameter for particles of 3.5 GeV/c central momentum. The design acceptances are ±3% in relative momentum and 100 π mm.mrad in transverse space. In addition to the injection-ejection equipment, the ring contains not less than seven stochastic cooling systems, one (Δp) acting on the injected beam, three (Δp, H, V) on the low density part or "tail" of the stored beam and three (Δp, H, V) on the high density part or "core" of the beam. Its layout is drawn in Fig. 20. The most striking feature is the great number of field-free straight sections. The ring consists of two superperiods and has the symmetry of the ellipse. In each quadrant, there are three FODO cells with a missing magnet dispersion suppressor corresponding to the scheme 3.1 (section 4.3)

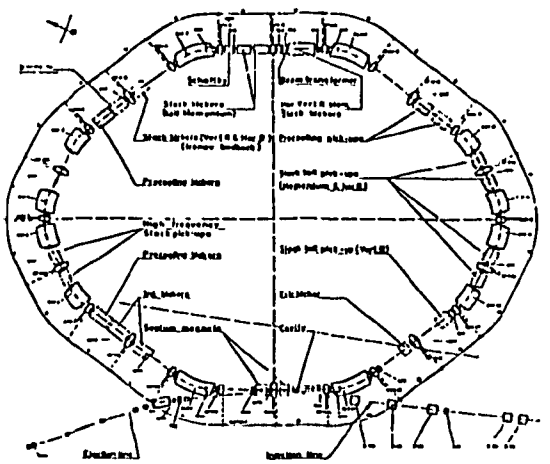

Fig. 20 Layout of the $\bar{p}$ accumulator.

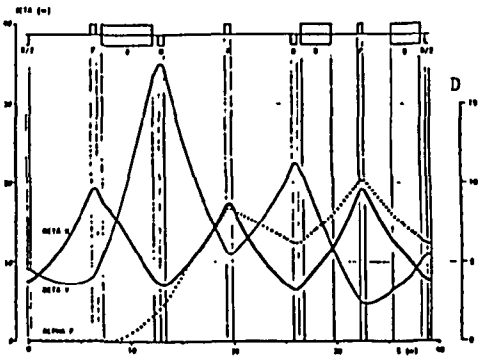

Fig. 21 Lattice functions: β_h, β_v, α_p.

which requires a horizontal phase advance per cell of 67.76 degrees. The β- and D-functions are plotted in Fig. 21. The horizontal aperture of the vacuum chamber is deeply modulated and reaches 68 cm in its widest part. The high absolute value of η (0.1), which is necessary for the stochastic cooling, is obtained with a moderate focusing (section 4.1), η is negative. The chromatic corrections use three families of multipoles (Fig. 17) since there are three quantities to correct: horizontal and vertical chromaticities and the orbit dispersion in the "zero dispersion" straight sections.

The experience gained on already existing storage rings and especially on the ISR has permitted to define the parameters of the machine from the very beginning in a precise and rather rigid way. The magnets are essentially energized by three power supplies, one for the dipoles, one for the F-quadrupoles and one for the D-quadrupoles. In the practice of the operation, it was found convenient to adjust the tracking of the two types of dipoles with a special trim coil wound on the wide dipoles and to re-balance the current in some wide F-quadrupoles to avoid lethal systematic seventh-order non-linear resonances ($7Q = 16, \ldots$). The rest of the fine adjustments results from a careful shimming of the end faces of the quadrupoles[28]. A happy consequence of this method is the excellent reproducibility and reliability of the magnetic system.

REFERENCES

1. D. Möhl, G. Petrucci, L. Thorndahl, S. Van Der Meer, Physics and Technique of Stochastic Cooling, Physics Reports 58-2-1980.

2. N. Tokuda, H. Yonehara, T. Hattori, T. Katayama, A. Noda, M. Yoshizawa, Stochastic Cooling of 7 MeV Protons at TARN.

3. P.J. Channel, J. Appl. Phys. 52 (6), 1981, p. 3791.

4. S. Van der Meer, Stochastic Extraction, a Low Ripple Version of Resonant extraction, CERN/PS/AA/78-6, R. Cappi, W. Hardt, Ultra Slow Ejection with Good Duty Factor, Proceedings of the XI-th International Conference on High Energy Accelerators, Geneva, July 1980.

5. G.I. Budker, N. Dikansky, V.I. Kudelainen, I.N. Meshkov, V.V. Parchomchuk, D.V. Pestrikov, A.N. Skrinsky and B.N. Sukhina, Part. Accel. 7, 197 (1976).

6. B. Autin and G. Guignard, End Effects of the Electron Cooling Section on the Proton (Antiproton) Beam, Proceedings of the Aspen Workshop on Colliding Beam Physics at Fermilab (1977).

7. R. Foster, T. Hardek, D.E. Johnson, W. Kells, V. Kerner, H. Lai, A.J. Lenox, F. Mills, Y. Miyahara, L. Oleksiuk, R. Peters, T. Rhoades, D. Young and P.M. McIntyre, IEEE Trans. Nucl. Sci. NS28, 2386 (1981).

8. L. Hütten, H. Poth and A. Wolf, H. Haseroth, C.E. Hill and J.L. Vallet, The Status of the Electron Cooling Device for LEAR, Proceedings of the 12th International Conference on High-Energy Accelarators, August 11-16, 1983, Fermilab, Batavia, Illinois.

9. D. Möhl, This course.
F. Sacherer, Stochastic Cooling Theory, CERN/ISR/TH/78-11, 1978.

10. S. Van der Meer, Stochastic Stacking in the Antiproton Accumulator CERN-PS/AA/78-22, 1978.

11. A. Garren, Private communication.

12. Tevatron 1 Project, Design Report, September 1983.

13. P. Lefèvre, This course.

14. See for instance E. Keil, Single Particle Dynamics, Linear Machine Lattices, in "Theoretical Aspects of the Behaviour of Beam in Accelerators and Storage Rings" CERN 77-13, 1977.

15. B. Autin, Dispersion Suppression with Missing Magnets in a FODO Structure. Proceedings of the 1979 Particle Accelerator Conference, San Francisco, 1979 .

16. M. Veltman, SCHIP, CERN Programme Library (R 201).
P.M. Gygi-Hanney, Private communication.

17. B. Autin, Simultaneous Correction of Chromaticity and Orbit Dispersion in a Strong Focusing Machine. Proceedings of the XI-th Int. Conf. on High Energy Accelerators, Geneva. 1980.

18. S. Chen, S. Fang, C. Zhang, Chromaticity in Strong Focusing Accelerators and Storage Rings. Communications in Theoretical Physics, vol.1 N° 2, 245-253, 1982.

19. W. Hardt, J. Jäger, D. Möhl, A General Analytical Expression for the Chromaticity of Accelerator Rings. PS/LEA/Note 82-5, 1982.

20. B. Autin, R. Billinge, R. Brown, G. Carron, C. Johnson, E. Jones, H. Koziol, C. Leemann, T. Sherwood, S. Van der Meer, E. Wilson, Beam Optics Studies on the Antiproton Accumulator. Proceedings of the 1981 Particle Accelerator Conference, Washington, 1981.

21. A. Ando, K. Takayama, Synchrotron Oscillations with Very Small η. IEEE Transactions on Nuclear Science, Vol. NS-30, N° 4, 1983.

22. J. Mac Lachlan, Programme ESME, (private communication).

23. R. Hagedorn, Stability and Amplitude Ranges of two Dimensional non Linear Oscillations with Periodical Hamiltonian, CERN 57-1.
G. Guignard, The General Theory of all Sum and Difference Resonances in a three - Dimensional Magnetic Field in a Synchrotron, CERN 76-06 (1976).
L. Evans, This Course.

24. B.V. Chirikov, Phys. Rep. 52:263-379, 1979.

25. D.F. Escande, Primary Resonances do not overlap, in Intrinsic Stochasticity in Plasma, G. Laval and D. Gresillon, eds. Editions de Physique, Orsay, 1979.

26. M. Wiedemann, Programme Patricia, PEP-Note 220, 1976.
A. Wrulich, Programme Racetrack, Private Communication.
D.R. Douglas, A.I. Dragt, Programme Marylie, IEEE Trans. Nucl. Sci. NS-28, 2522, 1981.
K.L. Brown, C. Iselin, Programme Turtle, CERN 74-2, 1974.

27. Design Study of a Proton-Antiproton colliding beam facility, CERN/PS/AA 78-3, 1978.

28. B. Autin, A. Bellanger, R. Billinge, R. Brown, C.D. Johnson, E. Jones, R. Sherwood, H.H. Umstatter, Multipole fields in the Antiproton Accumulator Magnet System, Proceedings of the 7 th International Conference on Magnet Technology, Karlsruhe, 1981.